Physics Letters A ••• (••••) •••–•••

Contents lists available at ScienceDirect

Physics Letters A

www.elsevier.com/locate/pla

Investigations of physical aspects of spinel ABi_2O_4 (A=Zn, Cd) oxides via ab-initio calculations

M. Waseem [a], I. Mahmood [a], Muhammad Rashid [b,*], Irfan Qasim [c], A. Laref [d]

[a] Center for High Energy Physics, University of the Punjab, Lahore, 54000, Pakistan
[b] Department of Physics, COMSATS University Islamabad, 44000 Islamabad, Pakistan
[c] Department of Physics, Riphah International University, Islamabad, Pakistan
[d] Department of Physics and Astronomy, College of Science, King Saud University, Riyadh, 11451 Saudi Arabia

ARTICLE INFO

Article history:
Received 29 October 2018
Received in revised form 13 February 2019
Accepted 28 February 2019
Available online xxxx
Communicated by R. Wu

Keywords:
Ab-initio calculations
Spinel oxides
Structural stability
Indirect bandgap semiconductors
Thermoelectric behavior

ABSTRACT

This present study aims to unravel physical properties of spinel oxides in cubic phase represented by general empirical formula of ABi_2O_4 (A=Zn, Cd) using full potential lineralized augmented plane plus local orbital (LAPW+lo) method. The structural aspect of spinel oxides in cubic phase has been investigated by Perdew-Burke-Ernzerhof generalized gradient approximation (PBEsol-GGA). The thermodynamic stability of ABi_2O_4 is established by computing the cohesive energies. On the other hand, born stability standard which is based on Chapin's tensor analysis method revealed that the mechanical stability of the oxide compounds under considerations gives a stable cubic phase. For a better prediction of electronic and thermoelectric properties of these compounds, the modified Tran-Bhala Becke and Johnson (TB-mBJ) potential is used which revels very precise band gap. Other than these investigations, thermoelectric characteristics i.e., Wiedman-Tranz constant, See-back coefficient and power factor are calculated and it provides essential data for fabrication of thermoelectric devices.

1. Introduction

The empirical formula AB_2O_4 representing a spinel oxide is well known as numerous technologically important materials adopt this crystal structure. The spinel oxides constitute an interesting class of material whose physical characteristics are categorized as novel and promising materials, due to their diversity of potential applications ranging from electronic devices to their ability to be used as water splitting, gas sensing [1], transparent conducting oxides (TCO) [2,3] and photo-catalysis [4]. The AB_2O_4 spinel oxides are commonly known to exhibit wide band gap (E_g) and adopt a close packed cubic structure belonging to the space group # 227, Fd-3m. In this crystallographic structure, the (1/8, 1/8, 1/8) and (1/2, 1/2, 1/2) positions are occupied by cations A and B, respectively, whereas the O atoms surround these cations in tetrahedral and octahedral coordination. As a result, the A cation adopts a 2^+ charge state, while the B cation is trivalent. It has been established in literature that B site cations are geometrically frustrated and produce a specific lattice known as pyrochlore lattice [5–7]. These pyrochlore lattices are attributed in literature to unorthodox and alluring scientific characteristics demonstrating diverse scope of material aspects [8,9].

Several classes of AB_2O_4 spinel oxides have been reported in literature [10–12]. Among these classes the bismuth contain spinel oxides ABi_2O_4 (with A=Zn and Cd) are of great interest owing to their promise for device fabrication and application. It has been demonstrated in previous investigations that $ZnBi_2O_4$ is formed due to interaction of ZnO with oxides of bismuth trivalent cations, where the difference of interstitial radius between Zn and Bi is approximately 0.15 Å [13]. For zinc bismuth Nano-particles ($ZnBi_2O_4$) cubic spinel structure has already been reported by Vijay Kumar et al. [14] who used the citrate gel auto combustion technique for stable synthesis of $ZnBi_2O_4$ Nano-particles. Analogously, the crystallographic structure of $CdBi_2O_4$ is similar to $ZnBi_2O_4$. Although synthesis, structural characterization and various other properties of ABi_2O_4 have been reported, there is a scarcity of thorough and in-depth investigations regarding stability and thermoelectric response of these materials.

In this paper, we report the first-principles calculations performed for ABi_2O_3 spinel compounds for exploring the effect of changing A from Zn to Cd in order in terms of mechanical stability in cubic phase and their corresponding thermoelectric properties. These facts have inspired us to perform a comprehensive investigation concerning the mechanical and thermoelectric properties

* Corresponding author.
E-mail address: muhammad.rashid@comsats.edu.pk (M. Rashid).

https://doi.org/10.1016/j.physleta.2019.02.048
0375-9601/

of this novel class of materials in their cubic phase for exploring their promising device fabrication. The spinel oxides ABi_2O_4 (with A=Zn and Cd) have been investigated using density functional theory (DFT). We use the modified Tran-Bhala Becke and Johnson (TB-mBJ) [15] for exploring the electronic structure of these compounds since TB-mBJ potential provides information about similar compounds which is comparable to experimental observations and provides accurate approximation for addressing realistic technological applications of wide band gap compounds. Moreover, BoltzTrap code [16] is used to simulate thermoelectric response of ABi_2O_4 (A=Zn, Cd) spinel oxides.

2. Method of calculations

Spinel oxides investigations of stability, electronic and thermoelectric characteristics are carried out using Wein2k package [17]. The full-potential linearized augmented plane wave plus local orbital (FP-LAPW+lo) method which is implemented in Wien2k code is used. The exchange co-relation potential by solving Kohn-Sham equations reveals the stability of cubic structural phase in terms of Perdew Burke Ernzerhof (PBE-Sol) provided the generalized gradient approximation (GGA) technique [18]. However, band gaps revealed by this GGA are found to be quite underestimated and undervalued within the boundaries set by DFT. This shortcoming can be surpassed by integrating modified Tran-Bhala Becke and Johnson (TB-mBJ) exchange potential [15]. Becke and Jhonson not only suggested but also established modified Becke and Jhonsons potential from a semi-local exchange potential. This very amalgamates exchange potential and correlation of mBJ as well as generalized gradient approximation respectively yielding meticulous and conscientious wide bandgap semiconductors [19,20] and spinel oxides [21,22].

The core electrons states in FP-LAPW+lo are determined by considering relativistic solution of Dirac equation and relativistic approximation is exploited for valence electron states which forsaking spin orbit coupling. The 2.38, 2.35, 2.41 and 1.98 a.u., is considered be most appropriate values for R_{MT} (i.e. muffin tin radius) of Zn, Cd, Bi and O respectively. The maximum values for angular momentum is $l_{max} = 10$ considered inside the atomic sphere for expansion of wave function. Similarly, the longest vectors in forces expansion is set at $G_{max} = 16$ $(Ryd)^{1/2}$ for charge density. Uniforms Monkhosrte pack [23] k-mesh $12 \times 12 \times 12$ has been considered for irreducible Brillouin zone (IBZ). The expansion of wave function is authorized by the relation i.e., $K_{max} \times R_{MT} = 8$. In the relation $K_{max} \times R_{MT} = 8$, K_{max} symbolizes reciprocal lattice wave vector 'K' and its maximum permissible values, whereas R_{MT} symbolizes muffins-tin radii. This optimize structure are subjected to self-consistent iterative calculations and yield ground state characteristics only when the iteration converges for energy and charge to the value less than 0.00001 Ry and 0.0001 e, respectively.

Through quasi-harmonic Debye model [24], the thermodynamic properties are computed through the Gibbs function $G^*(V; P, T)$ which is given by:

$$G^*(V; P, T) = E(V) + PV + A_{Vib}[\Theta(V); T] \quad (1)$$

here, the total energy is represented by $E(V)$, V is the unit cell volume, P is the pressure, A_{Vib} is the vibrational term and $\Theta(V)$ denotes the Debye temperature.

At constant pressure and temperature, Gibb's function has been attained with respect to volume as under:

$$\left(\frac{\partial G^*(V; P, T)}{\partial V}\right)_{(P,T)} = 0 \quad (2)$$

while using equation (2), for the values of the specific heat capacity (C_V), which is itself a thermodynamic property at constant volume with thermal expansion coefficient (α) is constructed with the help of following equation:

$$C_V = 3nk_B\left[4D\frac{\theta}{T} - \frac{3\theta/T}{e^{\theta/T} - 1}\right] \quad (3)$$

$$\alpha = \frac{\gamma C_V}{B_T V} \quad (4)$$

where the calculation of γ, the Grüneisen parameter, is performed using:

$$\gamma = \frac{dIn\theta(V)}{dInV} \quad (5)$$

Using above model different thermal properties like heat capacity, Grüneisen parameter and thermal expansion have been calculated.

In order to find out transport properties of the spinels under consideration, Boltzmann theory along with the BoltzTraP [16,25] was applied under the constant relaxation time approximation. In order to achieve convergence in Brillouin zone, 2000 k-points have been utilized. To get direction independency, in our current calculations, Relaxation time (τ) has been treated as constant (10^{-15} s) within the carrier concentration and temperature range.

3. Results and discussion

3.1. Structural behavior

Generally, in order to determine and investigate the energy released from relaxed structures are optimized by differential contrasting of the unit cell. The spinel oxides of the empirical for ABi_2O_4 (A=Zn, Cd) comprised of face centered (FCC) cubic structure and associated with 227-Fd-3m space group (Fig. 1b). The spinel oxides unit cell is comprised of both cubic tetrahedral and octahedral structures. In case of tetrahedral cubic structures, the central position are occupied by A=Zn, Cd atoms and in contrast to tetrahedral structures, central position is occupied by Bi atom in octahedral structures. In both tetrahedral and octahedral crystal structures, ionic sites are always occupied by 32-oxygen atoms, cationic sites are divided between A and Bi, 8a sites of A cation and 16-d sites of B cations are occupied in case of octahedral structure. Due to stress and Hellman-Feynman forces interactions in the structures, the self-consistent total energy dictates the optimization of such geometrical structures. Thorough and precise evaluation of Kohn-Sham equations along with significant and suitable atomic relaxation in a unit cell yields these variables. These parameters, i.e. Hellman-Feynman interaction forces and an integral stress must be at minimum value for an ideal and optimum a relaxation state and considered minimum value of 0.03 eVA^{-1} and 0.05 GPa respectively [26]. Fig. 1a depicts the spinel oxides ABi_2O_4 (A=Zn, Cd) that are optimized in cubic phase. Murnaghan formalisms [27] yields lattice constant (a_0) and bulk modules (B_0) for maximum energy released at minimum occupied volume of a unit cell. The yielded lattice constants for spinel oxides compounds increase from $ZnBi_2O_4$ to $CdBi_2O_4$ and for yielded bulk modules for these spinel compounds is found to be decreasing respectively (see Table 1), which is due to cationic (Zn, Cd) contrast.

3.2. Thermodynamic and mechanical stability

Stability of oxides is one of the fundamental features and necessary for requisition for fabrication of devices. Cohesive energies, Debye temperature and specific heat capacity are basic parameters that are required for validation of thermodynamic stability for under consideration oxides. Similarly, Borns stability criteria are also obligatory parameters for establishing structural and mechanical stability. To examine the stability of spinels under consideration

Please cite this article in press as: M. Waseem et al., Investigations of physical aspects of spinel ABi_2O_4 (A=Zn, Cd) oxides via ab-initio calculations, Phys. Lett. A (2019), https://doi.org/10.1016/j.physleta.2019.02.048

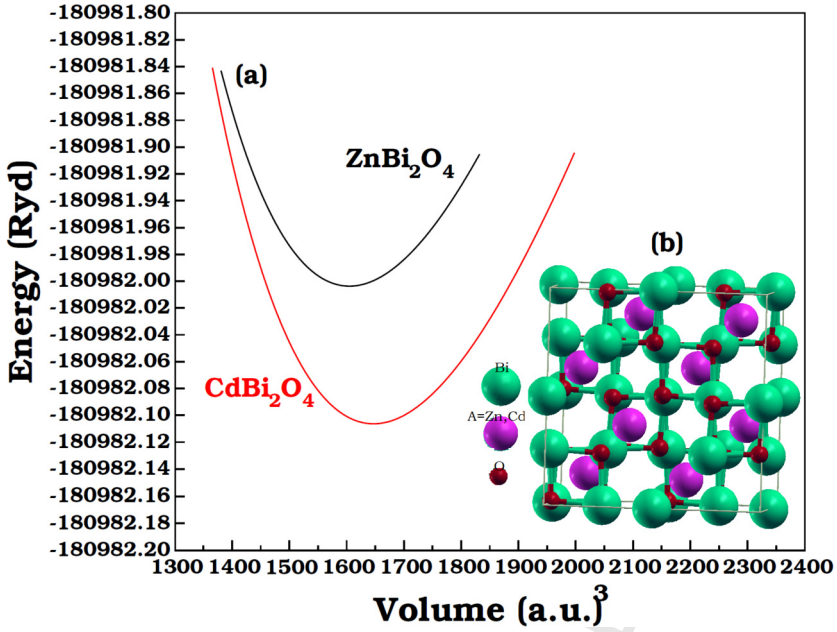

Fig. 1. (a) Energy versus volume plots using PBEsol-GGA for ABi_2O_4 (A=Zn, Cd) oxides and (b) the optimized cubic structure using Xcrysden Software.

Table 1
The calculated lattice constant a_0 (Å), bulk modulus B_0 (GPa), Cohesive Energy E_{coh} (eV), Elastic constant (C_{11} (GPa), C_{12} (GPa), C_{44} (GPa)), Shear modulus G (GPa), Young Modulus Y (GPa), Pugh ratio B/G, Average sound velocity υ_m (m/s) and θ_D (K) of $ZnBi_2O_4$ and $CdBi_2O_4$ spinels by using PBEsol-GGA approximation.

Parameters	$ZnBi_2O_4$	$CdBi_2O_4$
a_o (Å)	9.84	9.92
Other Cal.	9.65[a]	
B_0 (GPa)	113.97	113.08
E_{coh} (eV)	1.64	1.45
C_{11} (GPa)	232.94	246.68
C_{12} (GPa)	51.80	58.25
C_{44} (GPa)	29.65	37.42
B (GPa)	112.18	121.34
G (GPa)	47.29	54.27
Y (GPa)	124.39	142.67
B/G	2.37	2.27
υ	0.32	0.30
υ_ℓ (m/s)	6057.49	6194.6
υ_t (m/s)	3162.82	3269.8
υ_m (m/s)	3521.71	3676.2
θ_D (K)	322.9	311.9

[a] Ref. [43].

cohesive energies are computed which is the energy required to keep the atoms of any solid bound in order to retain the stability of the material. The calculation of cohesive energy is given as:

$$E_{coh} = (xE_A + yE_{Bi} + zE_{O_2}) - E_{Total}(A_xBi_{2y}O_{4z}) \quad (6)$$

where, total energy of the spinels is represented by $E_{Total}(A_xBi_{2y}O_{4z})$, while, E_A, E_{Bi}, E_{O_2} represent the ground state energies of the constituent atoms. It is clear from the spinels that the cohesive energy of is larger than that of their respective A=Zn/Cd. It is because the higher the chemical bond strength, the more the stability of the material will be [28]. The positive value of the cohesive energies is clearly shown in the Table 1 indicating structural stability. Energy releases during oxides formation state and its corresponding negative value as demonstrated in Table 1, establishes that these oxides formation occur in cubic phase. This can also be accounted from Table 1 that the cohesive energy for spinel oxides $ZnBi_2O_4$ is much more negative in comparison to $CdBi_2O_4$, thus stabling and corroborating the fact that stability increases as traversing down from Zn to Cd in group.

The elastic constants are yielded by solving first order non-linear differential equations of tensor matrix via Chapin technique [29]. Every aspect of mechanical stability is expressed using these yielded elastic constants foremost norm of inspecting mechanically stability is by Born stability criterion [30,31] i.e. $C_{11} - C_{12} > 0$, $C_{44} > 0$, $C_{11} + 2C_{12} > 0$ and $C_{12} < B_0 < C_{11}$. However, bulk modulus can be determined using following mathematical relation $B_0 = (C_{11} + 2C_{12})/3$. The calculated value bulk moduli are determined using optimized structures thus analogously these calculated value of mathematical relation yields veracious results. Additionally, ductility has major contribution in producing reliable and infallible devices as brittle devices can be easily broken, due to minor increase in stress. Thus ductile and brittle behavior analysis is mandatory and illustrated by Poisson's ratio (ν) and Pugh ratio (B_0/G). The boundary conditions for ductility and brittlity is mentioned in literature as $\nu > 0.26$ and $B_0/G > 1.75$ [32]. Materials are found to be ductile above this boundary limits and are found to be brittle below these limits. As these parameters are also listed in Table 1 and it can be easily concluded that these studied oxides are ductile in nature.

As it has been stated above thermodynamic stability depends upon not only on negative value of enthalpy of formation but also upon specific heat capacity which is linked to Debye temperature (θ_D). It yields information about heat tolerance of material. Following mathematical formula yield θ_D by solving tensor matrix of Charpin methods [33,34] and deduces its value as a function of sound velocity.

$$\theta_D = \frac{h}{\kappa_B}\left[\frac{3n}{4\pi}\frac{N_A\rho}{M}\right]^{\frac{1}{3}}\upsilon_m \quad (7)$$

where molar mass is represented by M. Avagadro's number by N_A, density by ρ and υ_m by density and average sound velocity. The longitudinal and transversal parts of Navior equations [35] can be utilized to determine average sound velocity via following relation.

$$\upsilon_m = \left[\frac{1}{3}\left(\frac{2}{\upsilon_t^3} + \frac{1}{\upsilon_\ell^3}\right)\right]^{-\frac{1}{3}} \quad (8)$$

where υ_t and υ_ℓ are the transverse and longitudinal velocity written from the relations.

$$\upsilon_t = \left(\frac{G}{\rho}\right)^{\frac{1}{2}} \quad \text{and} \quad \upsilon_\ell = \left(\frac{3B+4G}{3\rho}\right)^{\frac{1}{2}} \tag{9}$$

υ_t and υ_ℓ represents the transverse and longitudinal parts of Navior equations.

The findings are mentioned in Table 1 and it indicates a general trend of decreasing magnitude from $ZnBi_2O_4$ to $CdBi_2O_4$ because elasticity also drops in same manner. It is found that θ_D is in direct relation thus its value decreases from $ZnBi_2O_4$ to $CdBi_2O_4$. The θ_D is significant variable, provides inspiring insight about specific heat capacity (C_v) of under consideration materials as depicted in Fig. 2a. The specific heat capacity is found to be operating in conjunct ion with temperature and found to be increasing till 800 K which is due to free charge carriers and vibrations associated with lattice, both tend to increase with the temperature. The C_v of $CdBi_2O_4$ is higher than $ZnBi_2O_4$.

The characteristic plot of C_v is discussed in detail for higher temperatures ($C_v \propto T^3$) in literatures [36,37] and are found to be in accordance with Dulong-Petit law and Einstein model. However, for lower ranges of temperature results are found not to be in agreement with experimental results. The reasoning behind this disagreement and deviation is the dominance of acoustic phonons and lattice phonons vibrations are out of phase at lower temperatures. Debye proposed that these lattices vibrations are coupled together via immense number of frequency in comparison to isolated individual frequency. Table 1 and Fig. 2a demonstrates that specific heat capacity and Debye temperature are co-related. As Fermi-Dirac distribution is a function of temperature [38], both heat capacity (C_v) and electron density (n) derived in the present work from electronic structure calculations become a function of temperature. As increasing temperature are known to cause the electrons below the Fermi level to deplete, both the heat capacity and electron density of a material change with temperature. Through the calculation of specific heat capacity (C_v) and the carrier density (n) by keeping it at the constant volume, the thermodynamic behavior has been explored which has clearly been shown in Fig. 2a and Fig. 2b as well. The heat retained by the spinels and the heat absorbed are described by the specific heat capacity. The heat contributed by the both photons as well as electrons called net heat capacity is possessed by the semiconductors [$C_v = C_v(\text{phonon}) + C_v(\text{electrons})$]. It thus appears to be most important for indirect band gap semiconductors. Following the Debye law $C_V \propto T^3$, T is the temperature with which the C_v is linearly increased reaching at higher temperature where C_v turns to be $C_v = 3R$, in which the gas constant is symbolizes as R as shown in Fig. 2a. The computation of the electrons density (n) that has been set against temperature has been shown in Fig. 2b. With the increase in the temperature, the carriers are thermally excited which causes the increase in n. Since, specific heat capacity is also dependent on n and is inversely proportional to one another as displayed in Fig. 2b.

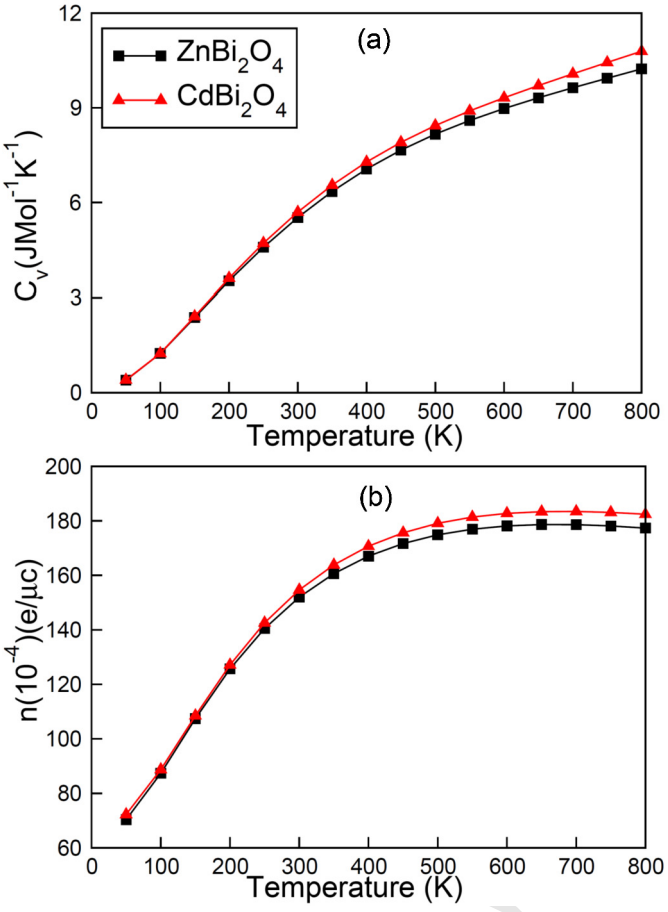

Fig. 2. Calculated (a) The Specific heat capacity and (b) number electron density of ABi_2O_4 (A=Zn, Cd) oxides plotted against temperature.

3.3. Electronic properties

In order to describe and understand electronic properties in elaborate manners band gaps and density of states are plotted for spinel oxides i.e. ABi_2O_4 (A=Zn, Cd) in Fig. 3 (a, b). It is evident from these plots studied oxides exhibits indirect bandgap in first BZ at high symmetry points investigational data are registered in Table 2, principally all electronics states are completely filled below the Fermi level and all the electronic states are vacant above the Fermi level where the Fermi level is set at zero. Shift in the conduction band minima is recorded away from Fermi level that

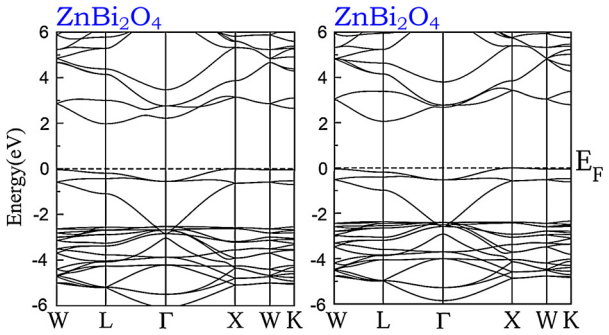

Fig. 3a. The calculated band structures of ABi_2O_4 (A=Zn, Cd) oxides by using mBJ potential.

Table 2
The calculated bandgap E_g (eV) and room temperature values of electrical conductivity (σ), thermal conductivity (κ) and See-beck coefficient (S), power factor (σS^2) and figure of merit (ZT) of $ZnBi_2O_4$ and $CdBi_2O_4$ oxides.

Spinel oxides	E_g (eV)	σ ($\times 10^{19}/\Omega$ m s)	κ_e ($\times 10^{14}$ W/mKs)	S (μV/K)	PF ($\times 10^{11}$ W/mK^{2}s)
$ZnBi_2O_4$	1.93	0.60	1.04	210.12	2.67
$CdBi_2O_4$	1.98	0.58	1.01	209.50	2.58

Please cite this article in press as: M. Waseem et al., Investigations of physical aspects of spinel ABi_2O_4 (A=Zn, Cd) oxides via ab-initio calculations, Phys. Lett. A (2019), https://doi.org/10.1016/j.physleta.2019.02.048

also ensures the shift in bandgap appear visible portion of EM spectrum. This observable shift is due to replaceable elements (A) in under consideration spinel oxides and this shift opens up new possibilities for potential applications in optoelectronic and solar cell fields. The observations recorded and as shown in Fig. 3a for states in valance bond conduction band. The states are found to be flat for valance band maximum and curved for conduction band minimum which endeavors ionic character and strong covalent character for understudy spinel oxides respectively. Thus general examination of these plots reveals the partial covalent character for spinel oxides. As, it has been clearly demonstrated that oxygen $2p$ states are assertive at 0 to 6 eV, 6 s Bi states are in conduction band and p states of Zn/Cd in Fig. 3b for total density of sates (TDOS).

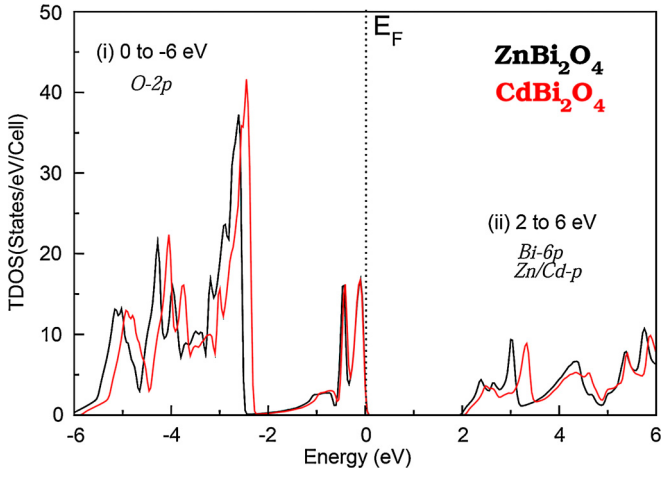

Fig. 3b. The total density of states (TDOS) along with partial density of states (PDOS) calculated for ABi_2O_4 (A=Zn, Cd) oxides by using mBJ potential.

3.4. Thermoelectric properties

The temptations to developed and design electrical power generator, which can recycle its wasted heat energy have led the pioneers and researchers in this specific field for couple of decades. The motivation behind this temptation is because of diminishing energy sources day by day. Thermoelectric processes provide an appropriate perspective, as it converts heat energy directly into electrical [39]. The currents of charge carries and phonon vibrations are the main sources of gradient deviations of heat energy and thus, producing potential difference. Based on these principles, thermoelectric devices are integrated in refrigerators and other power generating devices. The Fermi-Dirac distribution is a function of temperature [38] and the Boltzmann transport equations [16,25] utilize distribution function to compute the thermoelectric behavior of spinels. Electrical and thermal conductivities, power factors and See-back co-efficients are parameters to interpret thermoelectric behavior indispensable.

These parameters are predetermined versus span of temperature gradient ranging from 0 to 800 K for spinel oxides ABi_2O_4 (A=Zn and Cd). Fig. 4(a) is illustration of determined electrical conductivities of under considered spinel oxides plotted against temperature. The electrical conductivities for $ZnBi_2O_4$ and $CdBi_2O_4$ at 200 K are 0.42×10^{19} $(\Omega\,m\,s)^{-1}$ and 0.40×10^{19} $(\Omega\,m\,s)^{-1}$ respectively. As these values distinctively demonstrated that the decrease in electrical conductivity from Zn to Cd. At 800 K, the electrical conductivity for $ZnBi_2O_4$ and $CdBi_2O_4$ are 1.3×10^{19} $(\Omega\,m\,s)^{-1}$, 1.22×10^{19} $(\Omega\,m\,s)^{-1}$ respectively. This indicates an increase in electrical conductivities as temperature increases. It quite fascinating, there are decreases in electrical conductivities for Zn to Cd cations for the positive temperature gradient. This is due to positive change in metallic character from Zn to Cd cations, which is also in harmony to bandgap analysis as it also decrease due to rise in metallic character. Heat transference in materials are by thermal conductivities and in accordance to Fourier's law,

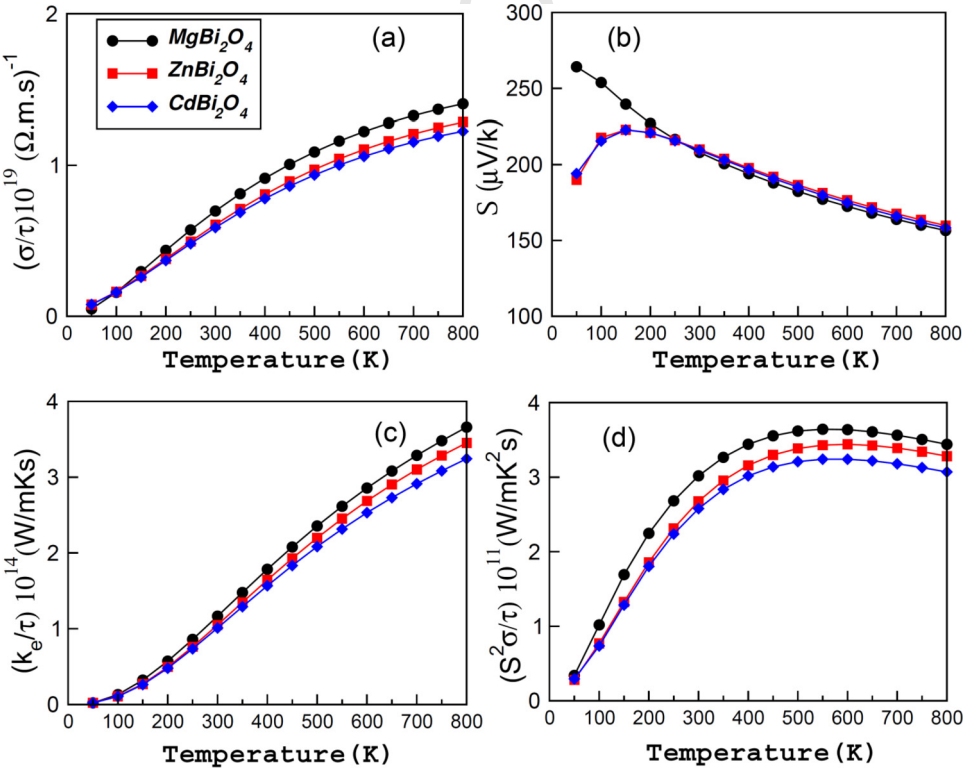

Fig. 4. Calculated (a) electrical conductivity, (b) See-beck co-efficient, (c) thermal conductivity, and (d) power factor plotted against temperature 100–800 K of ABi_2O_4 (A=Zn, Cd) oxides by using BoltzTraP code.

Please cite this article in press as: M. Waseem et al., Investigations of physical aspects of spinel ABi_2O_4 (A=Zn, Cd) oxides via ab-initio calculations, Phys. Lett. A (2019), https://doi.org/10.1016/j.physleta.2019.02.048

$q = -k\frac{dq}{dx}$ and for unit time and unit area thermal energy is express by k. Overall thermal energy of material consist of lattices vibrations i.e. phononic (k_l). Total thermal conductivity k ($k = k_l + k_e$) is composed of phononic (k_l) and the electronic (k_e) parts. In case of metals phonon associated thermal energy is minimal and thus neglected however both thermal energies are very significant in semiconductors. For spinel oxides ABi_2O_4 (A=Zn and Cd), the plot of electric thermal conductivities against temperature is shown in Fig. 4(c). It is evident from the plot, that at low temp the electronic thermal conductivity is also quite low but it steadily increases with the rise in temperature. At 200 K, the calculated value of electronic thermal conductivity for $ZnBi_2O_4$ and $CdBi_2O_4$ are 0.54×10^{14} W/mKs and 0.49×10^{14} W/mKs, respectively. The determine value is at its upper limits at 800 K. Thus, these spinel oxides have a subdued prospective for TE devices applications.

See-back coefficient (S) is also known as thermoelectric power and is exhibited in Fig. 4b. The free carries distinctiveness is represented by the positive or negative sign of See-back coefficient in the understudied material. Materials which are inherently rich in electrons (n-type) are assigned negative S, while material with holes or free carries are assigned positive S [40]. Generally free carries transfer themselves from material region with higher temperature towards the material regions with lower temperature and establish current because of potential difference. It has been established that S are generally tended to reduce for wide band gap semi-conductor. Analysis of $ZnBi_2O_4$ and $CdBi_2O_4$ yields that the magnitude of S dropped from common points.

Thermal efficiency can be deduced from thermal conductivity and See-back coefficient. Basically thermal efficiency can be calculated by taking simple product of square of thermal conductivity and See-back coefficients thus known as power factor (PF) [41,42] and calculated values of PF are listed in Fig. 4d. As, it can be summarized by considering Fig. 4d PF of spinel oxides ABi_2O_4 (A=Zn and Cd) increases with the rise in temperature till 800 K tangential derivatives of curve for $CdBi_2O_4$ is much lower than that of $ZnBi_2O_4$ respectively due to its thermal conductivity lower value. Among the studied spinel oxides, $ZnBi_2O_4$ has the highest PF since its thermal conductivity has the highest value. Investigational data regarding electrical and thermal conductivities, See-back coefficient, PF at room temperature are recorded and displayed in Table 2.

4. Conclusion

The investigations of stability, electronic and thermo-electric characteristics of spinel oxides ABi_2O_4 (A=Zn and Cd) are determined by using Wein2k simulation tool kit, which is based on FP-LAPW+lo techniques with DFT. Studied spinel oxides thermodynamic stability, structural and mechanical stability has been established by determined negative values of enthalpy of formation, Goldschmidt tolerance factors unity and mechanical stability by Born's criterion. Electronic band structure plots studied oxides exhibits indirect bandgap and shift in the conduction band minima is recorded away from Fermi level that also ensures the shift in bandgap appear invisible region. Thermal efficiency improvement has been also confined from Zn to Cd in the order due to increase in electrical conductivity. Entire analysis and study demonstrates that spinel oxides are substantially preferable for energy yielding and generating device applications

Acknowledgements

The author A. Laref acknowledges the financial support by a grant from the "Research Center of the Female Scientific and Medical Colleges", Deanship of Scientific Research, King Saud University.

References

[1] H. Kawazoe, K. Ueda, J. Am. Ceram. Soc. 82 (1999) 3330–3336.
[2] A. Stadler, Materials 5 (2012) 661–683.
[3] Z. Chen, C. Lu, Lett. 3 (2005) 274–295.
[4] C.G. Anchieta, D. Sallet, E.L. Foletto, S.S. da Silva, O. Chiavone-Filho, C.A.O. do Nascimento, Ceram. Int. 40 (2014) 4173–4178.
[5] X.L. Duan, D.R. Yuan, F.P. Yu, Inorg. Chem. 50 (2011) 5460–5467340.
[6] R. Ianos, S. Borcanescu, R. Lazaau, J. Chem. Eng. 240 (2014) 260–63342.
[7] S. Sumathi, A. Kavipriya, Solid State Sci. 65 (2017) 52–60.
[8] V.V. Ivanov, V.M. Talanov, V.B. Shirokov, M.V. Talanov, Inorg. Mater. 47 (2011) 990–998.
[9] P.W. Anderson, Phys. Rev. 102 (1956) 1008.
[10] A.K. Kushwaha, Compos. Mater. Sci. 85 (2014) 259–263.
[11] D. Allali, A. Bouhemadou, S. Bin-Omran, Comput. Mater. Sci. 51 (2012) 194–205.
[12] Saima Ali, M. Rashid, M. Hassan, N.A. Noor, Q. Mahmood, A. Laref, Bakhtiar Ul Haq, Physica B, Condens. Matter 537 (2018) 329–335.
[13] K.K. Khristoforov, I.G. Portnova, Y.A. Omel'chenko, et al., Glass Ceram. 37 (1980) 39.
[14] K. Vijay Kumar, CH. Shilpa Chakra, K. Rama Krishna, A. Rajesham, IJNR 2 (2017) 5.
[15] A.D. Becke, E.R. Johnson, J. Chem. Phys. 124 (2006) 221101.
[16] G.K. Madsen, D.J. Singh, Comput. Phys. Commun. 175 (2006) 67–71.
[17] P. Blaha, K. Schwarz, G.K.H. Madsen, D. Kvasnicka, J. Luitz, WIEN2K, an Augmented Plane Wave Plus Local Orbitals Program for Calculating Crystal Properties, Techn. Universität Wien, Austria, 2001.
[18] Z. Wu, R.E. Cohen, Phys. Rev. B 73 (2006) 235116.
[19] M. Hassan, N.A. Noor, Q. Mahmood, B. Amin, Curr. Appl. Phys. 16 (2016) 1473–1483.
[20] B. Sabir, N.A. Noor, M. Rashid, F.U. Din, S.M. Ramay, A. Mahmood, Chin. Phys. B 27 (2018) 016101.
[21] B. Amin, R. Khenata, A. Bouhemadou, I. Ahmad, M. Maqbool, Physica B, Condens. Matter 407 (2012) 2588–2592.
[22] M. Khan, S. Muhammad, B. Amin, Comput. Condens. Matter 13 (2017) 72–76.
[23] H.J. Monkhorst, J.D. Pack, Phys. Rev. B 13 (1976) 5188.
[24] M.A. Blanco, E. Francisco, V. Luania, Comput. Phys. Commun. 158 (2004) 57.
[25] T.M. Bhat, D.C. Gupta, RSC Adv. 6 (2016) 80302.
[26] A. Bouhemadou, R. Khenata, F. Zerarga, Eur. Phys. J. B 56 (2007) 1–5.
[27] F.D. Murnagham, Proc. Natl. Acad. Sci. 30 (1944) 244.
[28] Yu Feng, Ting Zhou, Xiaorui Chen, Hongkuan Yuan, Hong Chen, J. Magn. Magn. Mater. 38 (2015) 118.
[29] J. Young, J.M. Rondinelli, J. Phys. Chem. Lett. 7 (2016) 918–922.
[30] F. El Haj Hassan, H. Akbarzadeh, Comput. Mater. Sci. 38 (2006) 362.
[31] X. Ji, Y. Yu, J. Ji, J. Long, J. Chen, D. Liu, J. Alloys Compd. 623 (2015) 304–310.
[32] Q. Mahmood, M. Hassan, J. Alloys Compd. 704 (2017) 659–675.
[33] L. Fast, J.M. Wills, B. Johansson, O. Eriksson, Phys. Rev. B 51 (1995) 17431.
[34] O.L. Anderson, J. Phys. Chem. Solids 24 (1963) 909.
[35] E. Schreiber, O.L. Anderson, N. Soga, Elastic Constants and their Measurements.
[36] M. Marathe, A. Grunebohm, T. Nishimatsu, P. Entel, C. Ederer, Phys. Rev. B 93 (2016) 054110.
[37] M.A. Wahab, Solid State Physics, Structure and Properties of Materials, second edition, ISBN 1842652184, 2005, p. 596.
[38] C. Kittel, Introduction to Solid State Physics, Wiley, 1986.
[39] J. Zhang, Transport Studies of the Electrical, Magnetic and Thermoelectric Properties of Topological Insulator Thin Films, Vol. 99, Springer, 2016.
[40] D. Vasileska, S.M. Goodnick, Nano-Electronic Devices, Vol. 47, Springer Science and Business Media, 2011.
[41] H.C. Wang, W. Su, J. Liu, C.L. Wang, J. Materiomics 2 (2016) 225–236.
[42] X. Zhang, L.D. Zhao, J. Materiomics 1 (2015) 92–105.
[43] J. Saal, S. Kirklin, M. Aykol, B. Meredig, C. Wolverton, Materials design and discovery with high-throughput density functional theory: the open quantum materials database (OQMD), JOM 65 (11) (2013) 1501–1509.

Please cite this article in press as: M. Waseem et al., Investigations of physical aspects of spinel ABi_2O_4 (A=Zn, Cd) oxides via ab-initio calculations, Phys. Lett. A (2019), https://doi.org/10.1016/j.physleta.2019.02.048